ELSEVIER

Contents lists available at ScienceDirect

Carbohydrate Polymer Technologies and Applications

journal homepage: www.sciencedirect.com/journal/carbohydrate-polymer-technologies-and-applications





Effects of fatty acid esters on mechanical, thermal, microbial, and moisture barrier properties of carboxymethyl cellulose-based edible films

Sohini Mukherjee ^a, Avery Sengupta ^b, Subham Preetam ^c, Tanmoy Das ^d, Tanima Bhattacharya ^{e,*}, Nanasaheb Thorat ^{f,*}

- ^a Department of Environmental Science, University of Calcutta, 35 Ballygunge Circular Road, Kolkata 700019, West Bengal, India
- ^b Department of Food and Nutrition, University of Kalyani, Nadia, Kalyani, Pincode-741235, West Bengal, India
- ^c Department of Robotics and Mechatronics Engineering, Daegu Gyeongbuk Institute of Science & Technology (DGIST) Daegu, 42988 South Korea
- ^d Faculty of Engineering, Lincoln University College, Petaling Jaya 47301, Selangor Darul Ehsan, Malaysia
- ^e Faculty of Applied Science, Lincoln University College, Petaling Jaya 47301, Selangor Darul Ehsan, Malaysia
- f Department of Physics, Bernal Institute and Limerick Digital Cancer Research Centre (LDCRC), University of Limerick, Castletroy, Limerick V94T9PX, Ireland

ARTICLE INFO

Keywords: Carboxymethyl cellulose Cetyl-caprylate Cetyl-caprate Glycerol Plasticizer

ABSTRACT

Fatty acid esters being biodegradable and environment friendly has been a sought-after class of molecule for various food grade applications. This work involves the incorporation of fatty acid esters namely cetyl-caprylate and cetyl-caprate in edible Carboxymethyl cellulose -based films. The esters were enzymatically synthesized by esterification of caprylic acid and capric acid respectively with cetyl alcohol at a molar ratio of 1:1, using Candida antarctica lipase B which was immobilized (10 % w/w) at 65 °C. Carboxymethyl cellulose films were prepared. To it, glycerol and by emulsification, cetyl-caprylate or cetyl-caprate esters were amalgamated. Film characterizations involved analysis of surface morphology, mechanical properties, and thermal properties. It was further characterized by X-Ray diffraction analysis, water vapor permeability, and moisture uptake. Barrier property carboxymethyl cellulose films showed significant improvement due to the incorporation of cetyl-caprylate or cetyl-caprate esters. However, when the film's melting point was measured, it was seen that glycerol influenced the thermal properties more prominently than cetyl-caprylate and cetyl-caprate esters. Thus, the addition of an optimized amount of glycerol and cetyl-caprylate or cetyl-caprate esters to the carboxymethyl cellulose films is required for improved mechanical strength and better thermal properties. Further, an antimicrobial well diffusion assay of both the esters established the antimicrobial property of the same, which thereby recommends the addition of the wax esters even more.

1. Introduction

With the growing environmental concerns over non-biodegradable materials, the demand and concern for developing edible films from environment-friendly, biodegradable materials have seen a sharp rise in recent years (Karami et al., 2023). Several classes of biopolymers like proteins, polysaccharides, lipids, etc. have been used singly or in combinations for the preparation of edible coatings or films. One such abundantly available renewable biopolymer resource is cellulose (Helmiyati et al., 2021; Karami et al., 2023). Edible films based on cellulose derivatives have been reported to exhibit low water content and efficient barrier properties against oxygen and various aroma compounds. Various cellulose derivatives including methylcellulose (MC), hydroxyl

propyl methylcellulose (HPMC), and carboxymethyl cellulose (CMC) are reported to form continuous matrixes. Being readily water-soluble these types of esters of cellulose have no adverse effects on human health (Karami et al., 2023; Vilas Boas & de Castro, 2022). Various industries like cosmetics, food, pharmaceuticals, paper, textile, etc., are therefore using these films widely to improve the process and product quality (Roy & Rhim, 2020). Considerable work has been done involving MC and HPMC's behavior in film-forming. However, not much has been reported about CMC based films- film-forming and physical properties. Only effect of murta (Ugnimolinae Turcz) leaves extract has been studied (Vilas Boas & de Castro, 2022).

Efficient film-forming properties, thermal gelation, and rigorous oxygen and lipid barrier properties are exhibited by CMC. This makes it an excellent choice for extensive use in various food and pharmaceutical

E-mail addresses: btanima1987@gmail.com (T. Bhattacharya), nanasaheb.d.thorat@ul.ie (N. Thorat).

https://doi.org/10.1016/j.carpta.2024.100505

^{*} Corresponding authors.

Abbreviation

CMC Carboxymethyl cellulose

CCAPL Cetylcaprylate CCAPR Cetylcaprate

WVP Water vapor permeability

industries (Rahman et al., 2021; Roy & Rhim, 2020). As per the study of Liu et al.2022, the effects of grafting a long-chain saturated fatty acid on the preparation of hydrophobic composite membranes, utilizing carboxymethyl cellulose and modified pectin, were investigated (Liu et al., 2022). The results consistently demonstrated that the inclusion of docosanoic acid likely contributed to enhancing the overall properties of the polysaccharide-based composite membranes, potentially extending their utility in food packaging applications. Currently, various modified cellulose derivatives such as nanocellulose, carboxymethyl cellulose

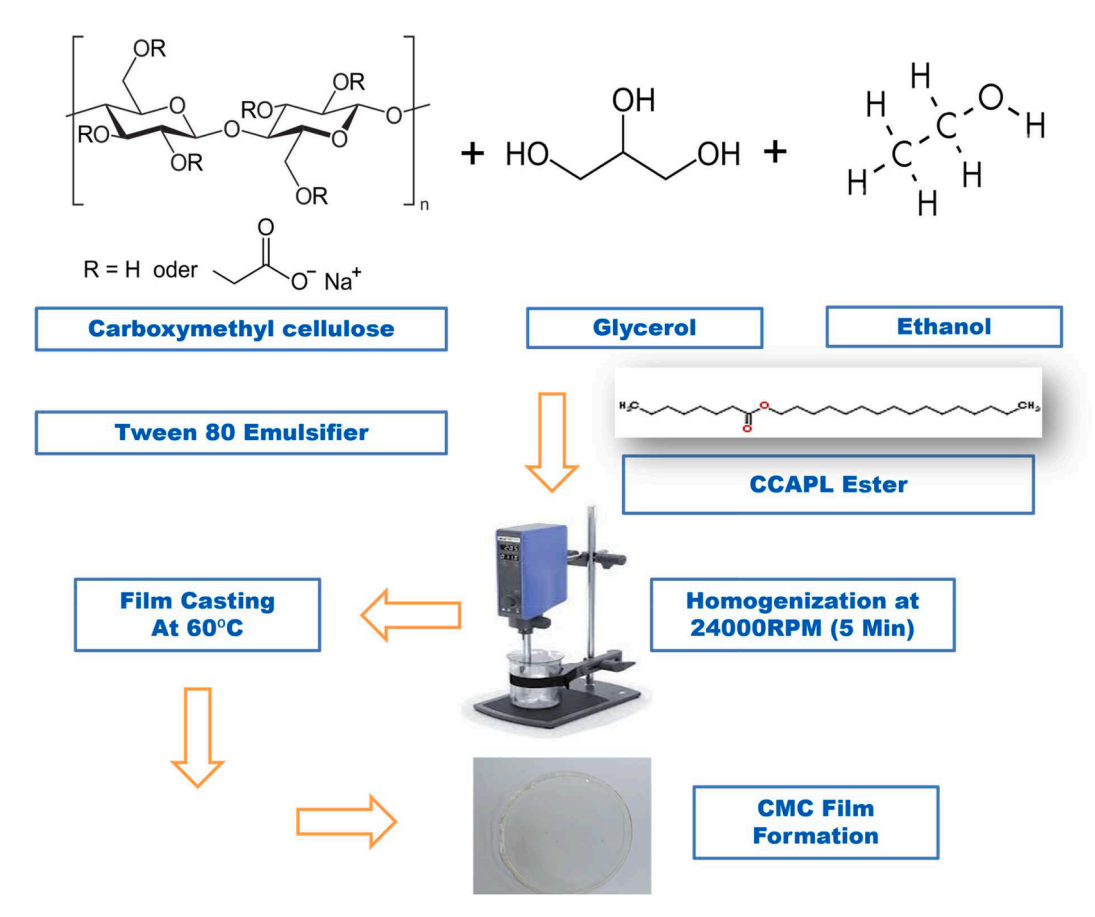


Fig. 1. Schematic diagram of process of cetyl caprylate (CCAPL) /cetyl caprate (CCAPR) ester plasticized CMC films. (For interpretation of the references to color in this figure legend, the reader is referred to the web version of this article.)

 Table 1

 CMC films compositions with or without plasticizer.

Samples	Sample Compositions				
	CMC (g)	Glycerol (ml)	CCAPL (ml)	CCAPR (ml)	Tween 80 (% of esters)
Pure CMC	1	0	0	0	0
Films					
(Control)					
CMC-GLY ^a	1	0.5	0	0	0
CMC-CCAPL1 ^b	1	0.5	0.3	0	1
CMC-CCAPL2	1	0.5	0.6	0	1
CMC-CCAPL3	1	0.5	0.8	0	1
CMC-CCAPR1 ^c	1	0.5	0	0.3	1
CMC-CCAPR2	1	0.5	0	0.6	1
CMC-CCAPR3	1	0.5	0	0.8	1

 $^{^{\}mathrm{a}}$ CMC-GLY- Carboxymethyl cellulose + glycerol.

 $\begin{tabular}{ll} \textbf{Table 2} \\ \textbf{Physical characterization of caprylic acid, CCAPLester, pure capric acid and CCAPR ester.} \end{tabular}$

Properties	Values			
	Caprylic acid	CCAPL ester	Capric acid	CCAPR ester
Flash Point (°C)	130 ± 0.05	Above 280	130 ± 0.47	Above 280
Viscosity (cP at	$5.~02\pm0.15$	4.82 \pm	4.372 \pm	4.02 \pm
40 °C)		0.025	0.1	0.15
Density (g/cm ³) at	0.904 \pm	0.844 \pm	0.894 \pm	$0.851~\pm$
30 °C	0.015	0.1	0.05	0.03
Slip Melting Point	20 ± 0.03	19.5 \pm	23 ± 0.02	21.5 \pm
(°C)		0.04		0.05

Values are represented as mean \pm SEM. n = 3.

(CMC), methyl cellulose, ethyl cellulose, and cellulose acetate have been successfully produced on an industrial scale. Among these, CMC and nanocellulose find extensive application in enhancing the gel properties of meat products. Studies have demonstrated that incorporating CMC

^b CMC-CCAPL- Carboxymethyl cellulose + cetylcaprylate ester.

^c CMC-CCAPR-Carboxymethyl cellulose + cetylcaprate ester.

Table 3FTIR peak assignment for cetyl alcohol, caprylic acid, CCAPL ester, capric acid and CCAPR ester.

Group of class	Range (cm ⁻¹)				
	Cetyl Alcohol	Caprylic Acid	CCAPL ester	Capric Acid	CCAPR ester
O-H and C-H stretching vibration	2910–2850	2900–3000	3300-2969.5	2922.8	2920.0-2850
O-H bending	1100	948–1419	940-1403	945-1418	943-1415
C-O stretching vibrations	1463- 719.7	1296	1468.9	1467-1353	1473.1 - 1326.2
C-O stretching vibration	_	1721	1712	1701	1732
C-H rocking vibration	1470–717	_	1465–709	_	1468-715
C-H bending	-	-	-	1218-456	1201-720

Table 4Antimicrobial activity of CCAPL and CCAPR against the test microorganisms.

Strains	Samples	ZoI (mm)
E. coli	Ampicillin	$1.\ 56\pm0.05$
S.aureus	Ampicillin	$1.70 \pm 0.02^{\rm a}$
E.coli	Glycerol	1.40 ± 0.05
S.aureus	Glycerol	Negligible ZOI
E.coli	CCAPL*	1.36 ± 0.02
S. aureus	CCAPL	1.96 ± 0.09^{b}
E.coli	CCAPR [#]	1.23 ± 0.02
S. aureus	CCAPR	$1.63\pm0.09^{\rm c}$

Values are represented as mean \pm SEM. n=3.Superscripts (a to c) indicate significance differences in results (p<0.05) between ZOI of esters [CCAPL and CCAPR] against *E.coli* and *S.aureus*.

into meat products can enhance their water retention capacity (Gibis & Weiss, 2017).

Pure carboxymethyl cellulose (CMC) indeed presents limitations such as low mechanical strength, thermal stability, gel fraction, and flexibility. To address these shortcomings, CMC can be combined with various other polymers, natural extracts, nanoparticles, enzymes, amino acids, and biomaterials. Methods such as grafting, chemical and physical cross-linking, radiation-induced blending, and coupling reactions are employed to modify CMC and enhance its properties. These modifications enable the development of CMC-based materials with improved mechanical strength, thermal stability, gel fraction, and flexibility, expanding their applicability across different industries (Aggarwal et al., 2024).

However, one drawback of this film is its poor resistivity toward water vapor transmission (Jannatyha et al., 2020). Nonetheless, the incorporation of lipid-based hydrophobic molecules into the film-forming solution can help boost its water vapor barrier values as it increases its hydrophobic/hydrophilic ratio. The high hydrophobicity of lipids blocks the moisture transport pathway across the film (Bozoğlan et al., 2020; Liu et al., 2022). It further protects the food surface from abrasion during handling and transport. The effect of different fatty acids on mango kernel starch has already been studied (Carvalho et al., 2021). Konjac glucomannan (KGM)-CMC blend films when impregnated with palm olein showed increased emulsion stability at the time of solvent removal by drying. The resultant films exhibited better barrier and mechanical characteristics (Liu et al., 2021). CMC-based films have emerged as promising contenders for food packaging applications. In a recent study, the efficacy of CMCs as a viable food packaging material was assessed by monitoring the vitamin C concentration and weight loss of red chillies. A comparison was drawn between samples stored without any film and those wrapped in CMC/CNC (cellulose nanocrystals) composite films at room temperature. Results indicated that the weight loss was significantly reduced in the CMC/CNC group compared to the non-film-wrapped group. This suggests that the films effectively mitigated moisture loss in red chillies due to their water vapor barrier properties. Furthermore, fresh chillies are known to contain high levels of vitamin C, which is prone to oxidation and degradation during

storage. The CMC composite films cross-linked with CNC exhibited the highest concentration of vitamin C and demonstrated superior gas barrier properties, indicating their potential to extend the shelf life and preserve the quality of food products (Tyagi & Thakur, 2023). In a noteworthy study, researchers investigated modified hydrogel films comprising blends of polyvinyl pyrrolidone (PVP) and CMC at various concentration ratios. Among these compositions, the hydrogel film with a 20:80 ratio of PVP to CMC exhibited superior elasticity modulus compared to other samples. These findings suggest that such hydrogel films have the potential to serve as a promising alternative for food packaging applications (Roy et al., 2010).

However, the amalgamation of hydrophobic components in the hydrophilic films may have hostile effects on various properties of the edible film, especially the mechanical and optical.

Fatty acids and their derivatives can also act as plasticizers in different biopolymer films (Mukherjee & Ghosh, 2017). Plasticizers when added to polymeric chains, aid in increasing the inter-molecular. This results in reduced brittleness, decrease in-situ forces, and increased flexibility and extensibility of polymers. Amongst the various studies carried out using various polyols on starch-based films, glycerol, sorbitol, and PEG seemed to be the most preferred ones (Paudel et al., 2023). In the case of edible films, glycerol is the most common plasticizer. The fatty acid esters of cetyl alcohol are known as wax esters which contain a good barrier property and have wide usage in the cosmetic industry. Reports on the use of these wax esters in various lubricants, plasticizers, polishes, and coating materials are available. But there has been no report on the application of fatty acid ester of cetyl alcohol as plasticizer into the CMC films (Yousuf et al., 2022). Thus, a balanced addition of both glycerol and fatty acid ester derivative in optimized proportions is required in the solution prepared for film formation This will help reduce the film's ability to transmit water vapor through it and also take care of any negative behavior of the mechanical and optical nature.

The present study deals with the lipase-catalyzed preparation of the cetyl alcohol esters of caprylic acid and capric acid by *Candida antarctica* with optimized process parameters. The esters were characterized by flashpoint, slip melting point, viscosity, and density analysis. Antimicrobial activity of the esters was also performed. Further, CMC/lipid composite films were developed using the technique of emulsification. The effect of cetyl-caprylate (CCAPL) and cetyl-caprate (CCAPR) ester on the mechanical, thermal, and crystalline properties was checked. The water barrier efficiency of the film was determined. Morphological properties of the film produced using glycerol-CCAPL/CCAPR plasticizers were also studied.

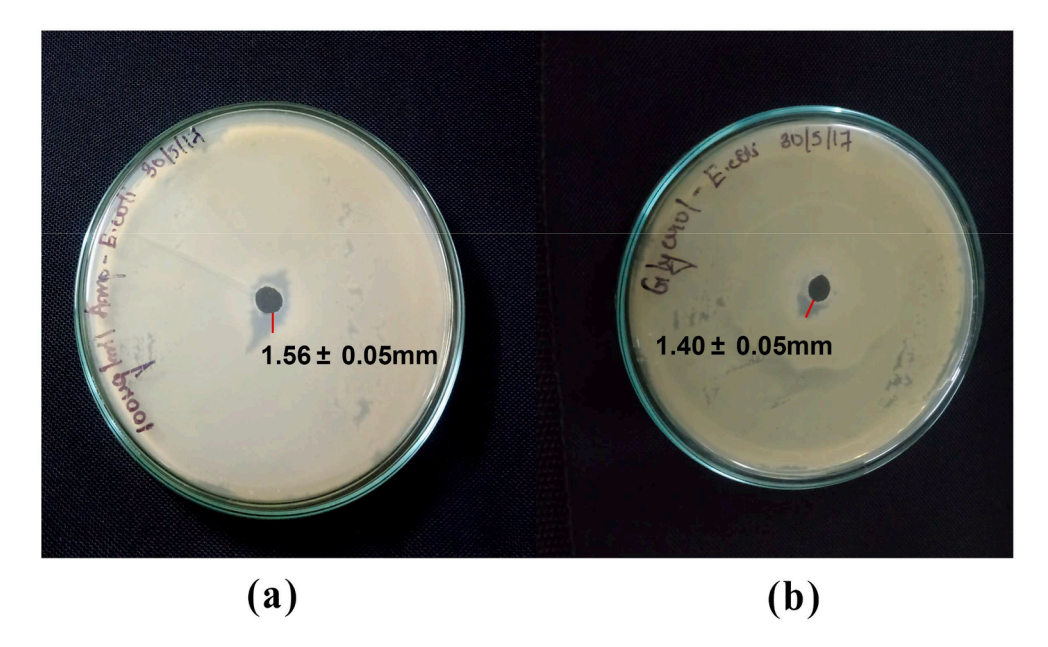
2. Materials and methods

2.1. Materials

Merck India Ltd. provided caprylic acid (C8:0) and capric acid (C10:0), which were purified using a gas chromatography (GC) apparatus. Loba Chemie in India provided the cetyl alcohol. Novozyme India Pvt. Ltd., Bangalore supplied the *Candida antarctica* immobilized lipase B (NS 435), *Thermomyces lanuginosus* immobilized (TLIM), *Rhizomucor*

^{*} CCAPR-Cetylcaprate.

[#] CCAPL-Cetylcaprylate.



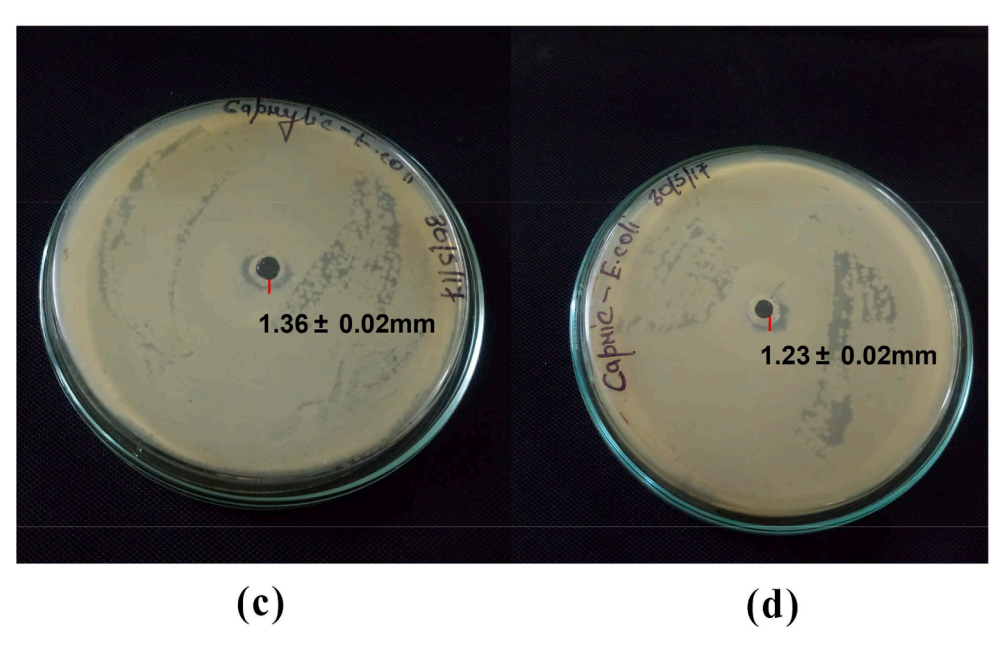


Fig. 2. Representative picture of inhibitory zones of *E.coli* against different edible plasticizers incorporated into the well diffusion plates. (a) Control (b) Glycerol (c) CCAPL (d) CCAPR. (For interpretation of the references to color in this figure legend, the reader is referred to the web version of this article.)

 $\it meihei$ immobilized (RMIM) used in this study. Merck, India Ltd. supplied carboxymethyl cellulose (CMC) (mol wt. 41,000 g/mol), analytical grade glycerol, and polysorbate 80 (Tween 80).

All other chemicals and solvents were of analytical grade and obtained from Merck, India Ltd.

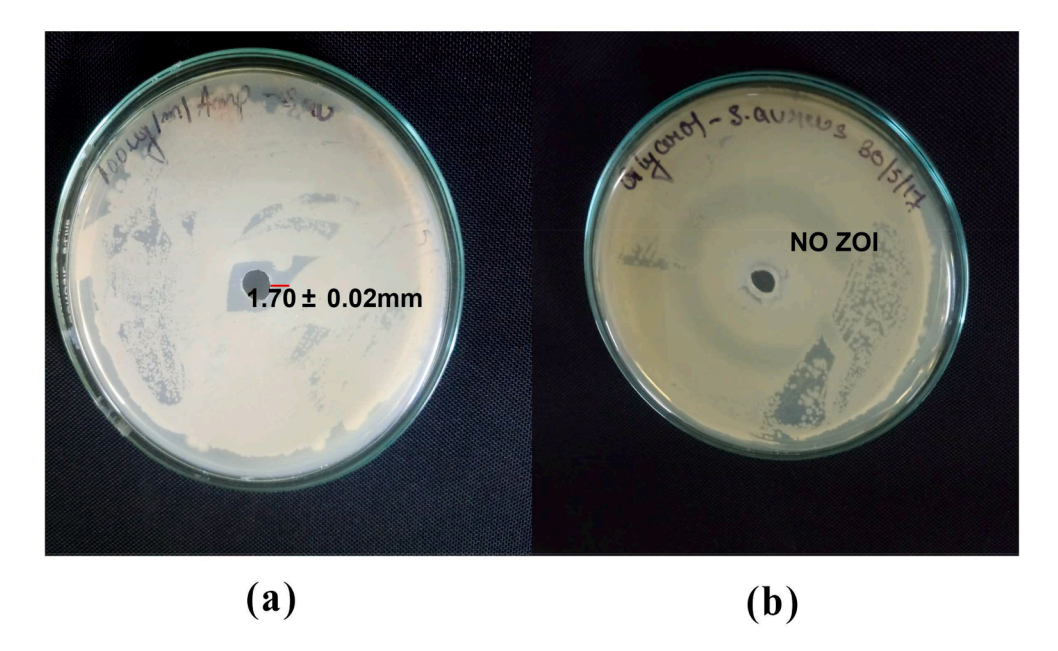
Microorganism and media component

Escherichia coli (k8813) and Staphylococcus aureus (ATCC 25,923) were provided by the Institute of Microbial Technology, Chandigarh, India. Nutrient agar slants consisting of gram per liter (g/l) of distilled water: peptone-10.00, agar-20, beef extract-10.00, sodium chloride (NaCl)–5, and pH 7.3 was prepared. The bacterial cultures were inoculated separately here incubated at 37 $^{\circ}$ C for 24 h in an incubator.

2.2. Method

2.2.1. Esterification reaction

To conduct the esterification of fatty acids with fatty alcohols (Caprylic acid:Cetyl alcohol and Capric acid:Cetyl alcohol), 1:1 molar ratios of each reactant were taken in two separate flat bottom flasks. Each of the reaction mixtures was stirred at 200 rpm, under vacuum (28 mm Hg) at 65 °C temperature with 10 % w/w of immobilized lipase (NS 435). No solvent was used in the reaction medium. After the alkali refining and steam distillation process, the reaction kinetics was confirmed by TLC. Spots confirming the presence of the ester formed and the absence of free fatty acid and alcohol used were checked. The entire reaction procedure has been provided in the schematic diagram Fig. 1 (Vide Figure S-1 and Figure S-2).



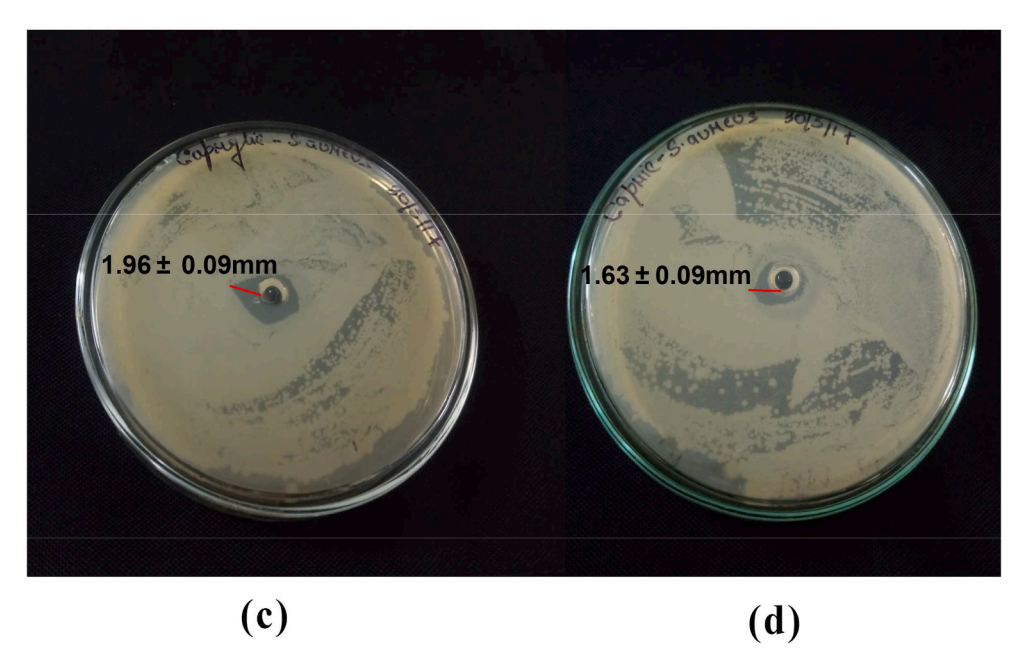


Fig. 3. Representative picture of inhibitory zones of *S. aureus* against different edible plasticizers incorporated into the well diffusion plates. (a) Control (b) Glycerol (c) CCAPL (d) CCAPR. (For interpretation of the references to color in this figure legend, the reader is referred to the web version of this article.)

2.2.2. Characterization of CCAPL and CCAPR esters

ASTM methods were followed for the determine of physical parameters such as density [ASTM D56–05], slip melting point [ASTM D 93–80], viscosity [ASTM D 445–04C2], and density [ASTM D891–2]. The products' Fourier transform infrared spectroscopy (FTIR) was recorded in the range $400–4000\ cm^{-1}$ using a Perkin Elmer Spectrum GX spectrophotometer.

2.2.3. Anti-microbial activity of cetyl-caprylate (CCAPL) and cetyl-caprate (CCAPR) by agar well diffusion method

Agar well diffusion method was practiced to determine the zone of inhibition required for determining the antimicrobial activity of the plasticizers (Roy & Rhim, 2020). 25 ml of agar was out into identical-sized glass petri plates and allowed to harden. Every plate agar surface was streaked with the reference bacterial strain using a sterile cotton swab. The Agar plate was perforated with a sterile 4 mm cork

borer, and 100 μl of each sample was poured into the hole with a micropipette. The plates were put on hold for 30 min.

The plates were kept aside for incubation for 24 h at 37 °C.

2.2.4. Preparation of films

Films were prepared as described by Ghanbarzadeh and Almasi (2011); with some modifications (Ghanbarzadeh & Almasi, 2011). CMC (1 g) and varying amounts of glycerol were dissolved in a solvent mixture of 33 ml water and 66 ml ethanol at about 60 °C (Table 1). After the addition of CCAPL and CCAPR separately in varying amounts and Tween 80 as emulsifier, the solutions were mixed and homogenized with an Ultra-Turrax T25 homogenizer at 24,000 rpm for 5 min Table 1. After cooling and removing air bubbles, each of the samples (50 ml) was poured into an even surface Petri plate, dried at 60 °C followed by casting. The films obtained were thin, homogeneous, flexible and transparent (Figure S-3 and Figure S-4).

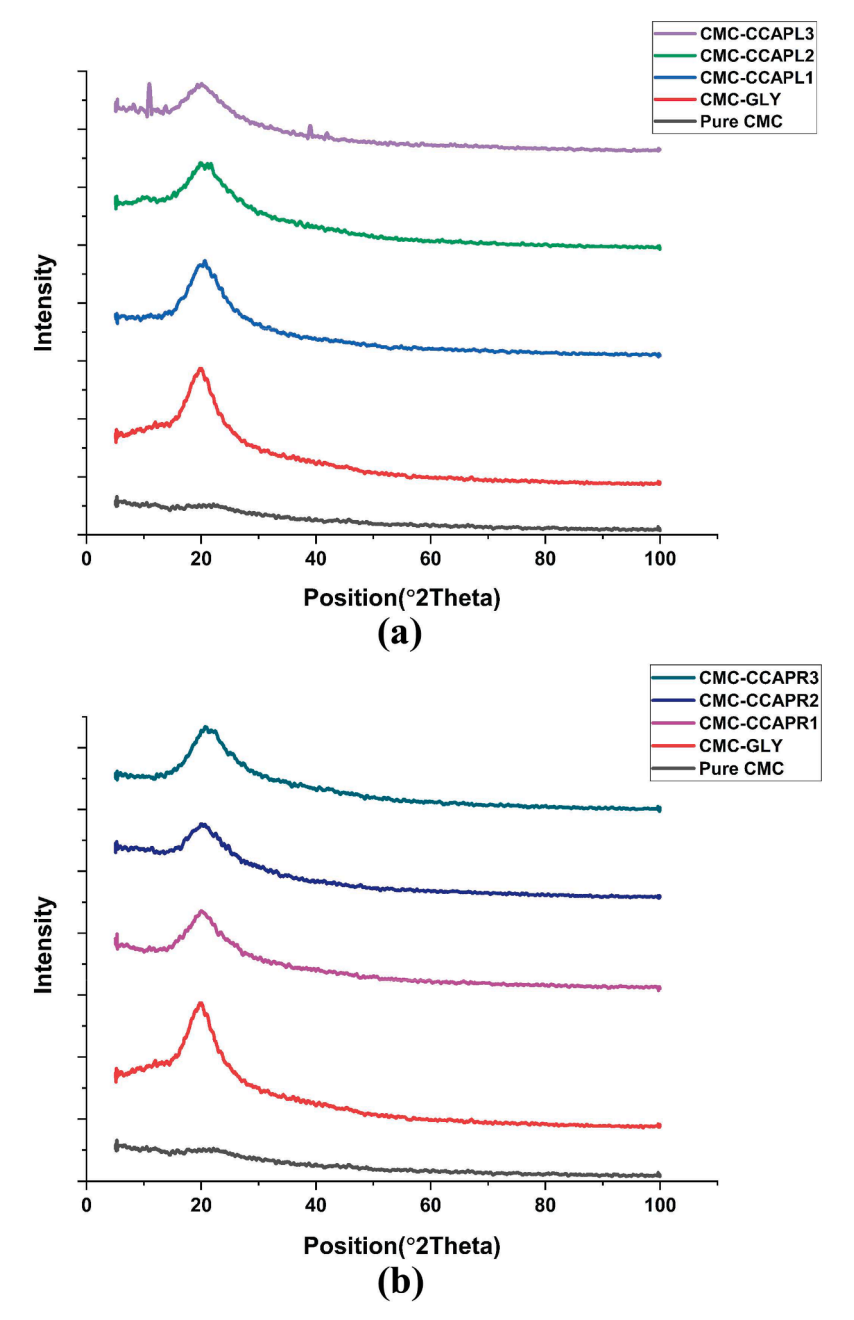


Fig. 4. (a) X-ray diffraction analysis of Pure CMC film, CMC film containing glycerol and CCAPL ester at different concentration. (b) X-ray diffraction analysis of Pure CMC film, CMC film containing glycerol and CCAPR ester at different concentrations. (For interpretation of the references to color in this figure legend, the reader is referred to the web version of this article.)

2.2.5. X-ray diffraction

To check if the addition of CCAPL and CCAPR ester and glycerol caused any alterations in the crystallinity of the films, they were subjected to X-ray diffraction following the method and instruments of Mukherjee et al., 2020 (Mukherjee & Ghosh, 2020).

2.2.6. Scanning electron microscopy (SEM)

A thin layer of Au was sputter-coated with CMC film samples to observe the SEM images. Thereafter, the coated samples were observed by Zeiss EVO 18 Special Edition (Germany) with 15 kV accelerating voltage in secondary electron mode. The magnification was 10 kX in SEM images (Mukherjee & Ghosh, 2017, 2020). Instruments and methods were used in accordance to Mukherjee et al. 2017 (Mukherjee & Ghosh, 2017).

2.2.7. Atomic force microscopy (AFM)

AFM was performed on Veeco di Innova (Bruker AXS Pvt. Ltd., USA) by placing the film samples onto the mica surface. All of the images were recorded in tapping mode by silicon cantilevers. Commercial probes were used with a spring constant of 20–80 N/m and a resonance frequency of 240–308 kHz. The scale in testing was 8.0 $\mu m \times 8.0~\mu m$. The software Nanoscope V1.40 was used to process the AFM images (Mukherjee & Ghosh, 2017). Through AFM measurements, it becomes feasible to compute parameters that define surface roughness. Rq (root mean square deviation from the mean) and Ra (arithmetical mean deviation from the mean) were determined from various line profiles.

2.2.8. Mechanical properties

A universal instrument of mechanical properties (Instron, 5565, USA) with a 50 N loaded cell was used for tensile strength, elongation at

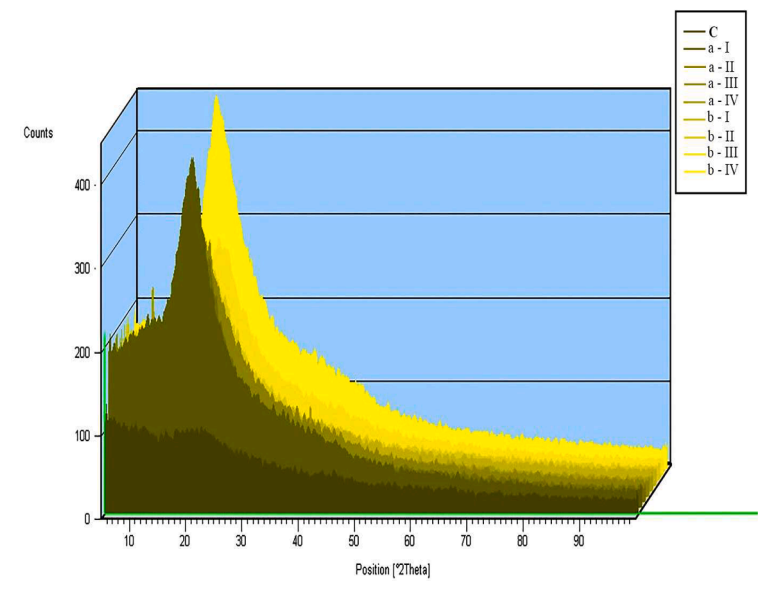


Fig. 5. X-ray diffraction (3D image) analysis of Pure CMC film (C=control), CMC film containing glycerol CCAPL (a-I to a-IV) and CCAPR (b-I to b-IV) ester at different concentration. (For interpretation of the references to color in this figure legend, the reader is referred to the web version of this article.)

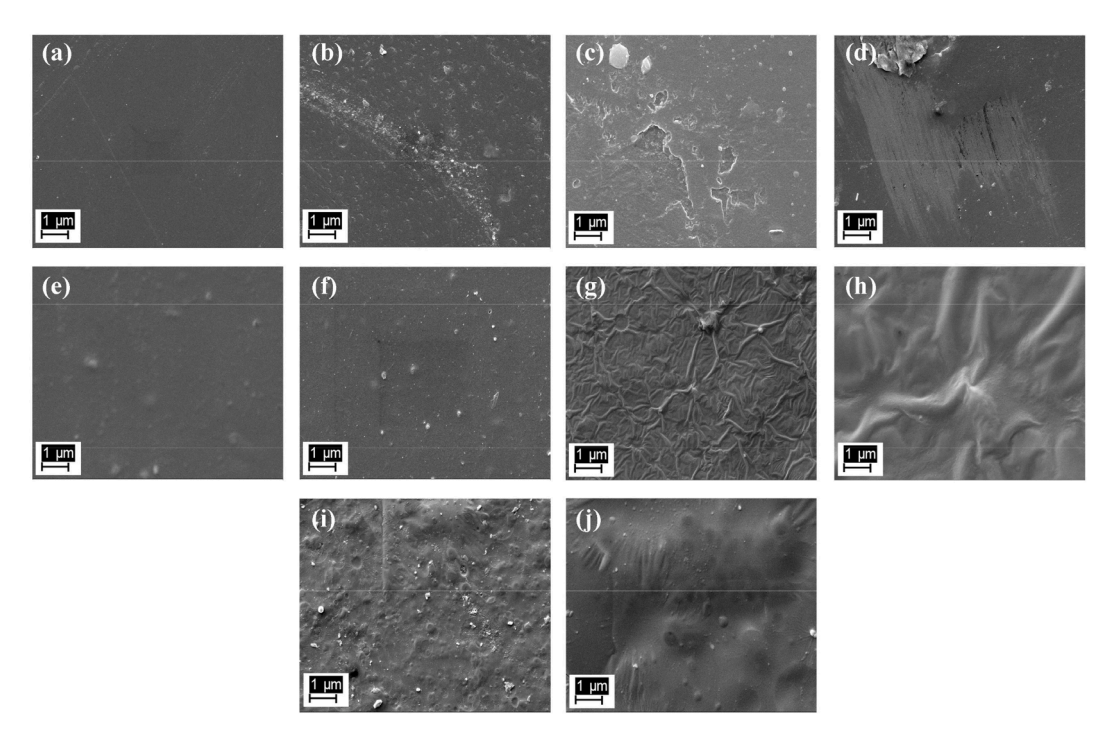


Fig. 6. SEM images of (a) Pure CMC film, (b) CMC film with Glycerol[CMC-GLY], (c to f) CCAPL ester[CMC-CCAPL1, CMC-CCAPL2, and CMC-CCAPL 3],(g to j) CCAPR ester [CMC-CCAPR1,CMC-CCAPR2, and CMC-CCAPR 3] as plasticizer.

break and elastic modulus testing in a constant extension speed of 5 mm/min. Three film specimens, 8×0.5 cm strips, were cut from each of the film samples and were mounted between the grips of the machine. The initial grip separation and cross-head speed was set to 50 mm and 5 mm/min, respectively (Mukherjee & Ghosh, 2020).

2.2.9. Thermogravimetric analysis, derivative thermogravimtry and differential thermal analysis (TG/DTG/DTA)

Thermogravimetric analysis (TG/DTG/DTA) was conducted using a Perkin Elmer thermal analyzer equipped with diamond thermogravimetric analysis and differential scanning calorimetry (TG/DTG/DTA) capabilities, controlled by Pyris software. The analysis was performed in

an aluminum pan under a nitrogen flow rate of 25 mL/min. The samples were heated from 20°C to 200°C at a rate of 10°C/min . Using the belowmentioned equation, the sample TGA was calculated:

Weight
$$loss(\%) = (Wi - Wf)/Wi \times 100$$
 (1)

Where, $W_i = \text{initial weight}$, $W_f = \text{final weight}$

The derivative form of TGA, known as DTG, is acquired by employing differentials of TGA values (Oun & Rhim, 2015). Additionally, differential thermal analysis (DTA) was carried out using the same Perkin Elmer Diamond TG/DTA thermal analyzer and Pyris software. The film samples, weighing approximately 5 mg, were scanned under nitrogen flow at 25 mL/min. Initially, the sample was preheated to

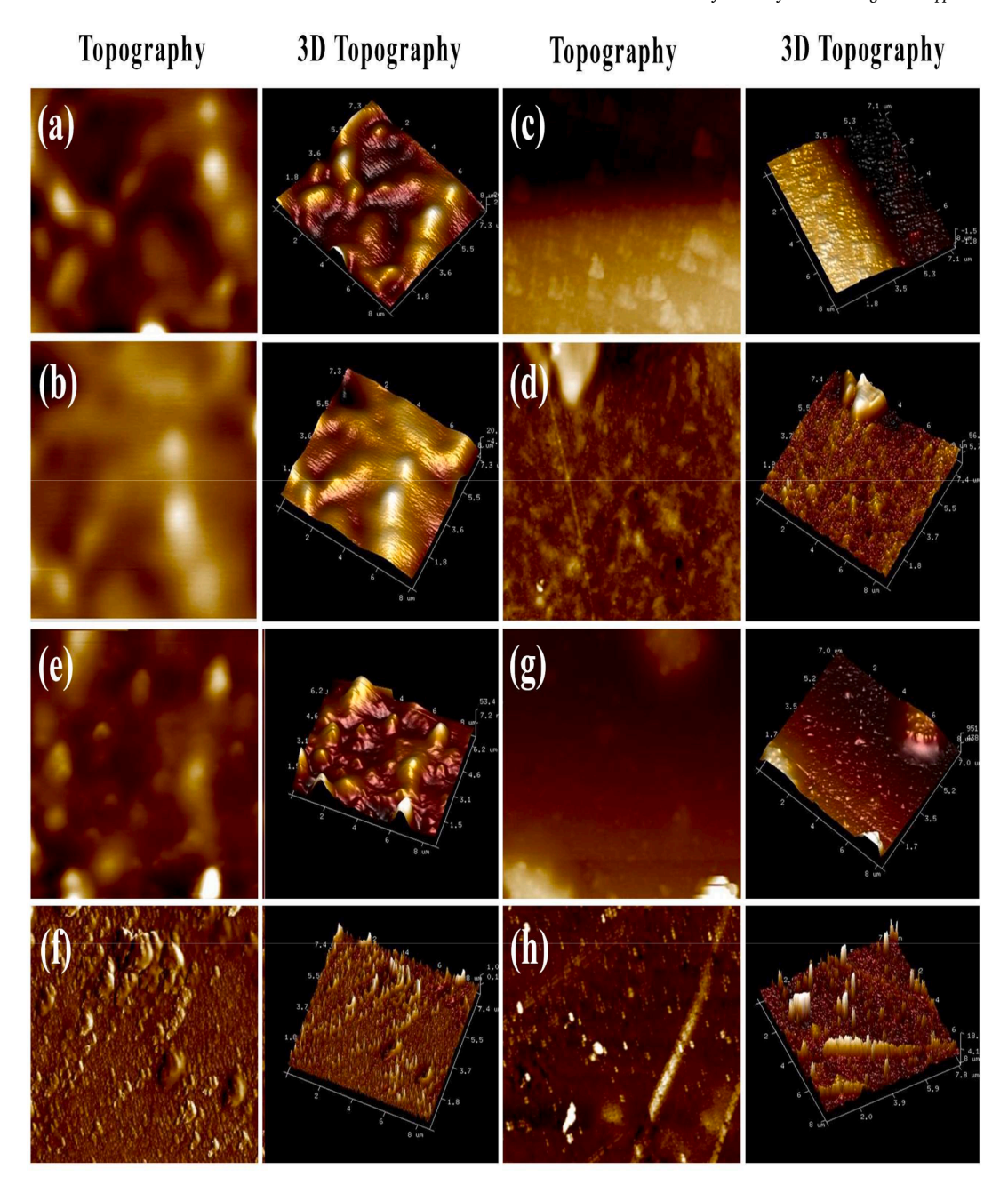


Fig. 7. AFM images of (a) Pure CMC film, (b) CMC film with Glycerol[CMC-GLY], (c to e) CCAPL ester[CMC-CCAPL1,CMC-CCAPL2, and CMC-CCAPL 3], (f to h) CCAPR ester [CMC-CCAPR1,CMC-CCAPR2, and CMC-CCAPR 3] as plasticizer. (For interpretation of the references to color in this figure legend, the reader is referred to the web version of this article.)

150°C at a rate of 20°C/min to remove water and eliminate thermal history. Subsequently, after cooling to 20 °C, the sample underwent a second scan, heating up to 200°C at a rate of 10° C/min Mukherjee and Ghosh (2017), 2020.

2.2.10. Water vapor permeability (WVP)

Using the ASTM E96–00 method (modified) WVP of the CMC films with and without plasticizer (CCAPL, CCAPR, and glycerol) was checked. A permeable container was filled with calcium chloride (0 % RH within the cell). It's opening of 60 mm diameter was sealed with the film sample. Next, a glass desiccator was filled with a saturated sodium chloride solution (75 % RH outside the cell). This resulted in a gradient throughout the film (Karami et al., 2023). Every 24 h, weight of the permeable container was checked until stable. The water vapor transfer rate was determined using Amin et al's equation Amin et al. (2012) as

done by Mukherjee & Ghosh (2017) Water vapor transmission rate was calculated by using the following equation:

$$Q = WL/S \tag{2}$$

where W is increase in the desiccant weight per 24 h, L is the film thickness (cm), S is the exposed surface area (cm 2) and Q is the water vapor transmission rate (g/cm 2 /24 h).

2.2.11. Moisture uptake

Post 48 h conditioning (0 % R_H due to presence of anhydrous CaSO₄ at) weight of CMC film samples (2 cm \times 2 cm) was taken and conditioned at 25°C. It was put in a desiccator with a saturated K_2SO_4 solution (developing an R_H of 97 %). Weight of all sample strips were checked after 48 h. Using the below-mentioned equation, the samples' moisture

Table 5Mechanical properties of CMC films with or without plasticizer.

Sample	Young's Modulus (MPa)	Tensile Strength (MPa)	Elongation at break (%)
CMC	580 ± 0.52	22.01 ± 0.15	6.70 ± 0.05
(control)			
CMC-GLY ^a	72.76 ± 1.09	13.12 ± 0.24	27.56 ± 0.14
CMC-	89.02 ± 1.59	9.86 ± 0.14	30.67 ± 0.13
CCAPL1 ^b			
CMC-	90.07 ± 0.99^{d}	4.37 ± 0.31	$35.09 \pm 0.28 \text{ g}$
CCAPL2			_
CMC-	70.08 ± 0.93	$2.09\pm0.21^{\rm f}$	45.09 ± 0.08
CCAPL3			
CMC-CCAPR	97.03 ± 2.09^{e}	9.65 ± 0.23	24.09 ± 0.10
1 ^c			
CMC-	79.53 ± 3.23	7.73 ± 0.32	29.80 ± 0.07
CCAPR2			
CMC-	90.41 ± 1.19	$5.17\pm0.19~\mathrm{g}$	$32.09 \pm 0.37^{\rm h}$
CCAPR3			

Values are represented as Mean \pm SEM. n=3.Superscrpits (d to h) indicate the significance differences in results (p<0.05) between mechanical tests of the films.

- $^{\mathrm{a}}\,$ CMC-GLY- Carboxymethyl cellulose + glycerol.
- ^b CMC-CCAPL- Carboxymethyl cellulose + cetylcaprylate ester.
- ^c CMC-CCAPR-Carboxymethyl cellulose + cetylcaprate ester.

uptake values were computed .:

moisture uptake% =
$$\frac{W - W_0}{W_0} \times 100$$
 (3)

where W = after 48 h of exposure to 97 %R_H, the weight of the film sample

 W_0 = the initial weight of the sample.

2.3. Statistical analysis

Triplicates (n=3) results are reported for all analyses. Standard errors (Mean \pm SEM) are reported with all data. One-way ANOVA was implemented for statistical comparisons among groups. Tukey test (using Origin Pro 8 software) was used to ascertain the level of significance p<0.05.

3. Result and discussion

3.1. Yield of the ester

Reaction parameter for maximum yield of CCAPL and CCAPR ester, the lipase being immobilized NS 435 (10 % w/w), was found at 6 h with the reactant molar ratio of 1:1 and 65°C reaction temperature. The data regarding the parametric dependence of both set of reactions has been provided in the supplementary file (Figure S-5 to Figure S-10)

3.2. Characterization of CCAPL and CCAPR ester

3.2.1. Physical characterization

Table 2 shows the physical characterization of pure caprylic acid, CCAPL ester, pure capric acid, and CCAPR ester. The results were comparable to the studies reported by others. The flashpoint was obtained above the 280°C in the case of both CCAPL and CCAPR ester. The viscosity of caprylic acid and CCAPL ester was 5.02 cP and 4.82cP respectively at 50°C. The viscosity of capric acid and CCAPR ester at 40°C was 4.372cP and 4.02 cP respectively. Density of CCAPL and CCAPR was almost similar when the values were compared with pure caprylic acid and pure capric acid respectively. The slip melting point of CCAPL ester was slightly lower than caprylic acid. The same phenomena were observed in the case of the slip melting point of the CCAPR when it

was compared with pure capric acid.

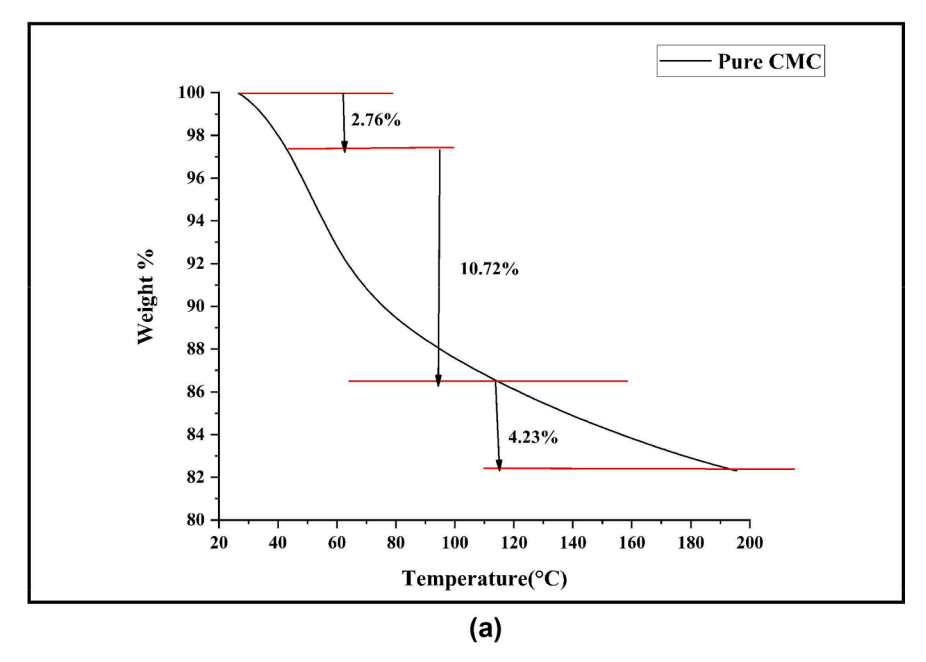
3.2.2. FTIR analysis of pure cetyl alcohol, caprylic acid, CCAPL, capric acid, and CCAPR ester

The absorption wavelengths of FTIR spectra of pure caprylic acid, cetyl alcohol, and CCAPL ester are presented in Table 3 and the spectrograms are given in the supplementary file [Figure.S-11 (a,b, and c)]. OH stretching band centering near 3000 cm⁻¹ is seen as abroad peak. Caprylic acid if present as a cyclic dimer can exhibit such a peak. Further, a medium intensity band at 1107 cm⁻¹ is observed. [Table 3, Figure S-11 a] An out-of-plane deformation of O...H...O hydrogen bond can be reported to be this [Chung, Kim, Jung, Kwak,2009]. C-H stretching (2500–3000 cm⁻¹), C-O stretching vibration (1712 cm⁻¹), and C-O stretching vibrations were found at several intensities in the FTIR spectra of caprylic acid (Table 3, Figure.S-11 a). Table 3 [Figure.S-11 (b)] described the FTIR spectra of cetyl alcohol. O-H stretching vibration (3325.1 cm⁻¹), C-H stretching vibration (2918.2 cm⁻¹), and C-O stretching (1463 cm^{-1}) , 1064.3 cm^{-1} , and 719.7 cm^{-1}) were observed in the case of the FTIR spectral analysis of cetyl alcohol. Table 3 [Figure.S-11 c] depicted the FTIR spectral analysis of the CCAPL ester. The O-H stretching vibration (3300 cm⁻¹), C-H stretching vibration (2969.5 cm⁻¹), C-O stretching vibration (1712 cm⁻¹), and C-O stretching vibration (1468.9) were observed at sharp intensities which confirmed the CCAPL ester formation.

The absorption wavelengths of FTIR spectra of pure capric acid, cetyl alcohol, and CCAPR ester are presented in Table 3 [Figure.S-12 (a, b, and c)]. Table 3 [Figure.S-12 (a)] describes the FTIR spectra of capric acid. O-H stretching vibration (2922.8 cm $^{-1}$), and C-O stretching vibration (1701 cm $^{-1}$) were observed in the case of FTIR spectra of capric acid. Table 3 [Figure.S-12 (b)] also describes the FTIR spectra of cetyl alcohol. O-H stretching vibration (3325.1 cm $^{-1}$), C-H stretching vibration (2918.2 cm $^{-1}$), and C-O stretching (1463 cm $^{-1}$,1064.3 cm $^{-1}$, and 719.7 cm $^{-1}$) were found to have occurred in the case of the FTIR spectral analysis of cetyl alcohol. FTIR spectra of the CCAPR ester (Figure.S-12 c) showed C-H stretching vibrations (2920.0 cm $^{-1}$), O-H stretching vibrations (2850.2 cm $^{-1}$), C-O ester stretching vibration (1732 cm $^{-1}$), C-O stretching vibrations (1326.2 cm $^{-1}$ to 1473.1 cm $^{-1}$), and C-H bending (720.0 cm $^{-1}$ to 1201 cm $^{-1}$) which confirmed the CCAPR ester formation [Bakry et al., 2017].

3.2.3. Anti-microbial activity of cetyl-caprylate and cetyl-caprate by agar well diffusion method

CCAPL and CCAPR esters were subjected to anti-microbial studies. Table 4. describes the CCAPL and CCAPR ester's antimicrobial activities. Representative pictures of inhibitory zones of both E.coli and S. aureus respectively against CCAPL and CCAPR ester are given in the supplementary file (Figs. 2a-d and 3a-d). Both CCAPL and CCAPR ester indicated a distinct zone of inhibition in both cases of S.aureus and E.coli. But both the esters exhibited better antimicrobial activity in the case of S. aureus in comparison to E.coli. These esters might be potential to the S. aureus. It is widely recognized that certain saturated fatty acids possess notable antibacterial properties against both Gram-positive and Gramnegative bacteria, suggesting their potential as alternatives for the development of new antibacterial agents (Ezati et al., 2023; Khan et al., 2023). Among the diverse array of saturated fatty acids, lauric acid stands out as a naturally occurring fatty acid with significant antibacterial activity. This compound has been extensively tested against various bacteria, demonstrating particularly strong effects on Gram-positive bacteria. When a 1:10 v/v dilution of lauric acid was applied, it showed growth inhibition against clinical isolates of Staphylococcus aureus and Streptococcus pneumoniae, resulting in inhibition zones of 15 mm. However, towards Mycobacterium tuberculosis, E. coli, and Salmonella spp., lauric acid displayed comparatively lower activity, with lesser inhibition zones (Balouiri et al., 2016; Basiak et al., 2018; Dashipour et al., 2015; Hashim & Hamad, 2018; Helmiyati et al., 2021).



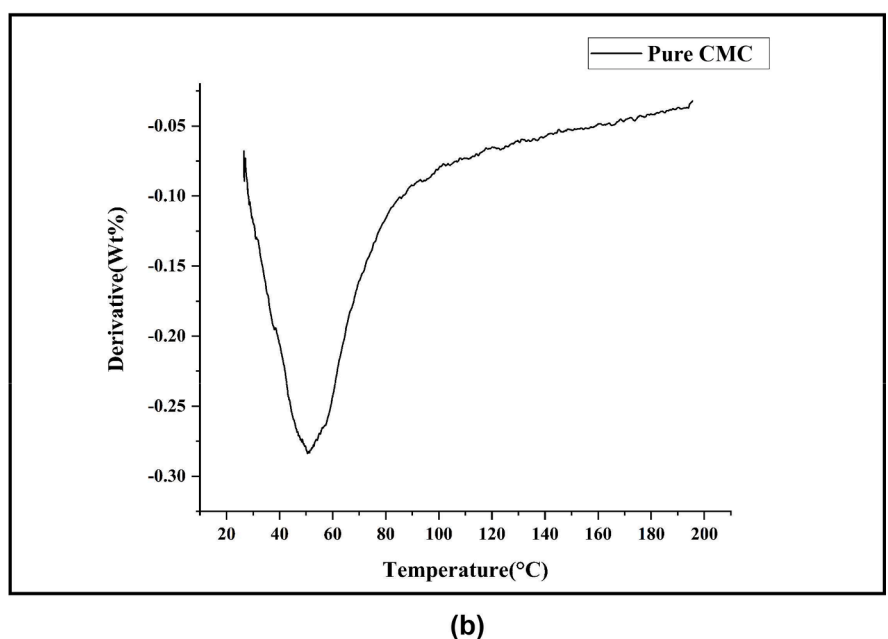


Fig. 8. (a) TG and (b)DTG curves of, pure CMC film. (For interpretation of the references to color in this figure legend, the reader is referred to the web version of this article.)

3.3. Film characterization

3.3.1. X-ray diffraction (XRD) analysis of the CMC films

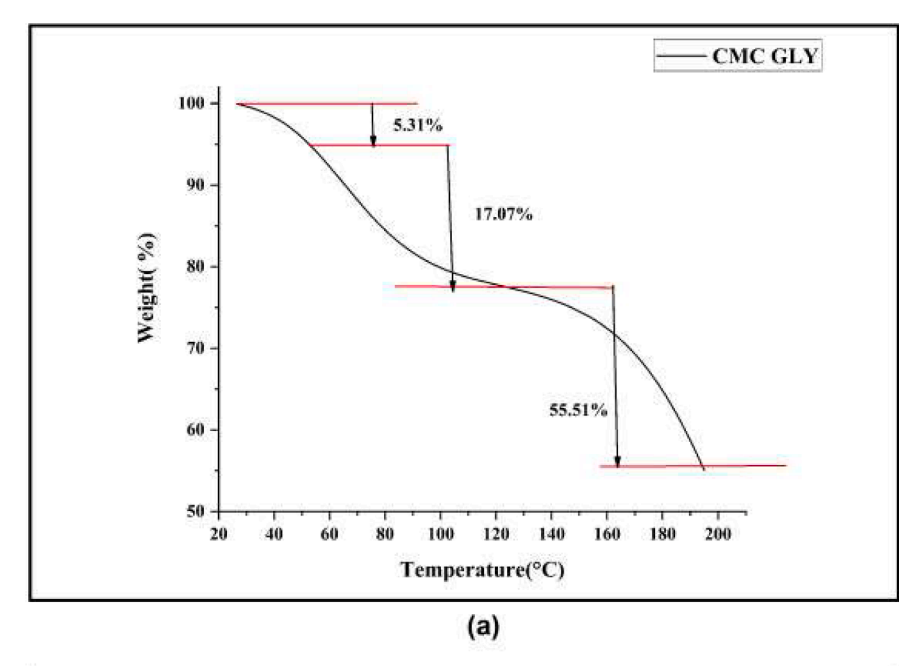
Film arrangement was determined by X-ray diffraction. Fig. 4 (a) and (b) explain the XRD patterns of pure CMC films, CMC films containing CCAPL and CCAPR as plasticizers respectively. Fig. 5 presented the 3D images of the XRD patterns of pure CMC films, CMC films containing different concentrations of CCAPL and CCAPR as plasticizers respectively. Glycerol was used as a conventional edible plasticizer. Fig. 4 (a and b) both shows the XRD pattern of pure CMC film which is amorphous but in the case of the CMC films containing glycerol as a conventional plasticizer (Fig. 4 a) shows a bell-shaped curve at 20° of 2 Θ position. The same patterns of curves were observed in Fig. 4 (a) when CCAPL was incorporated in the CMC films at a different concentration by replacing glycerol. Fig. 4 (b) shows the XRD patterns of pure CMC film (Fig. 4 b), CMC films containing glycerol as conventional plasticizer

(Fig. 4 b), and CMC films containing CCAPR ester at different concentration (Fig. 4 b) respectively. This Fig. 4 (b) also shows the same XRD pattern as the glycerol plasticized CMC films. Here CCAPL and CCAPR esters showed equivalent performances as glycerol.

3.3.2. Scanning electron microscopy

SEM images of pure CMC film, CMC films containing glycerol as a conventional plasticizer, CCAPL, and CCAPR respectively are shown in composite Fig. 6 (a-j). CMC films without plasticizers showed (Fig. 6) a smooth and plane surface whereas the CMC film with glycerol showed quite rough surface (Fig. 6 b). When CCAPL ester was introduced in place of glycerol in different proportions, the surfaces of the films seem smoother in comparison to the conventional glycerol plasticized films. Hence, CCAPL ester was quite miscible with CMC and glycerol.

SEM images of the CMC films containing CCAPR as the plasticizing agent are presented in Fig. 6 (g, h, i, and j). CMC film containing glycerol



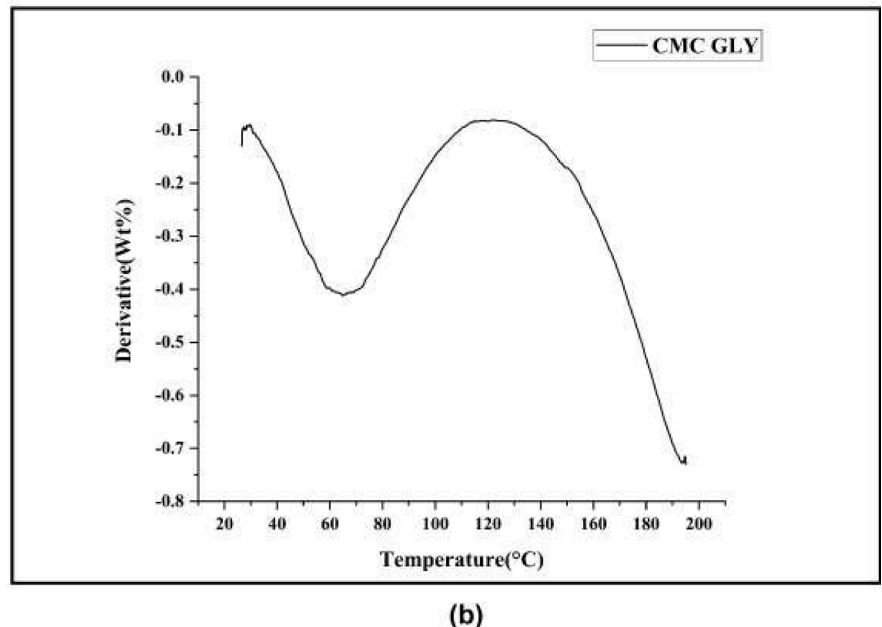


Fig. 9. (a) TG and (b)DTG curves of, pure CMC+GLY (glycerol) film. (For interpretation of the references to color in this figure legend, the reader is referred to the web version of this article.)

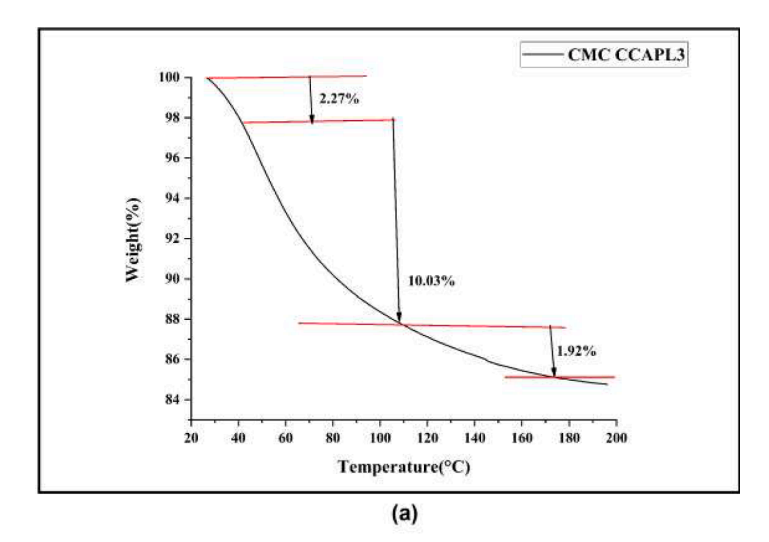
as a plasticizer in a large proportion and CCAPR at a minor proportion showed (Fig. 6 g, h) quite a rough surface in comparison to the pure CMC film (Fig. 6 a). But in the case of Fig. 6 (g, h), a different kind of surface is observed which may be generated due to the interaction between CMC, glycerol, and increasing concentration of CCAPR. Finally, a quite smoother surface is found in the case of Fig. 6 (i and j). This phenomenon might be due to the miscibility of CCAPR ester at a higher concentration with CMC and with the least proportion of glycerol (Bakry et al., 2017; Bozoğlan et al., 2020; Ghanbarzadeh & Almasi, 2011). Therefore, the SEM images (Fig. 6 a–j) of CMC films containing CCAPL and CCAPR as a plasticizer establish that these esters could be good replacements for conventional plasticizers. Better surface morphology was observed in the case of CCAPL ester-containing CMC films in comparison to CCAPR ester-containing films (Mukherjee & Ghosh, 2017, 2020; Nazrin et al., 2020).

3.3.3. Atomic force microscopy

To examine the surface morphology and roughness of pure carboxymethyl cellulose (CMC), as well as CMC films incorporating CCAPL and CCAPR plasticizers, atomic force microscopy (AFM) was utilized. The AFM images depicting the topography and 3D surface features are presented in Fig. 7 (a-h).

The AFM analysis of the pure CMC film (Fig. 7a) revealed a smooth surface with some nodular structures, consistent with findings from previous studies (Mukherjee & Ghosh, 2017; Zhu et al., 2020). Comparatively, the CMC-GLY film exhibited a rougher surface (Fig. 7b), with Ra and Rq values of 5.06 nm and 3.98 nm, respectively. The CMC films containing glycerol as plasticizer exhibited lower Ra and Rq value [Figure S-18 (a-g) Supplementary information]. Similar kind of results were found to be observed in several studies (Dmitrenko et al., 2023; Escamilla-García et al., 2022).

Notably, the CMC-CCAPL 1 film surface displayed uneven



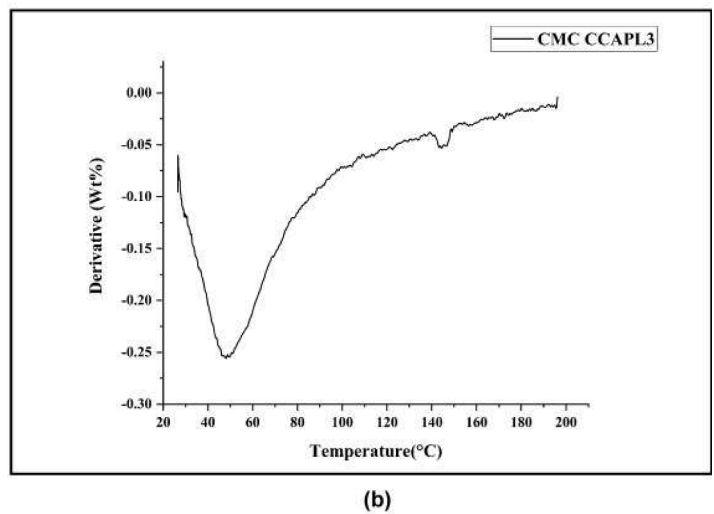


Fig. 10. (a) TG and (b)DTG curves of, pure CMC CCAPL3 film. (For interpretation of the references to color in this figure legend, the reader is referred to the web version of this article.)

distributions of nodular structures (Fig. 7c), possibly attributed to interactions between plasticizers and the CMC molecule. However, CMC-CCAPL 2 and CMC-CCAPL 3 films (Fig. 7d and e) showed smoother surfaces with increasing concentrations of CCAPL ester. In contrast, the Ra and Rq values of CMC-CCAPL 1 are 50.7 nm and 59.5 nm, respectively, whereas those of CMC-CCAPL 3 are 38.39 nm and 11.7 nm, respectively [Figure S-18 (a-g) Supplementary information]. The results showed lessere roughness at higher CCAPL ester concentration (Dmitrenko et al., 2023; Escamilla-García et al., 2022).

Conversely, AFM images of CMC films containing lower concentrations of CCAPR ester (CMC-CCAPR1 and CMC-CCAPR2) (Fig. 7f and g) displayed a distinct surface morphology, potentially due to molecular interactions among CMC, glycerol, and CCAPR ester. Notably, CMC-CCAPR 3 film (Fig. 7h) exhibited a smoother surface, indicating better compatibility of CCAPR ester at higher concentrations with CMC and minimal glycerol content (Dahlström et al., 2024). Hence, bio-polymeric films incorporating specific quantities of plasticizers may influence the formation of various bonds (Mukherjee & Ghosh, 2017; Zhu et al., 2020). The Ra and Rq values for CMC-CCAPR 1 are 5.50 nm and 7.20 nm, respectively, while for CMC-CCAPR 3, they are 4.52 nm and 5.94 nm, respectively. This suggests that the observed variations in surface morphologies in AFM images across different films could be attributed to differences in plasticizers' hydrophobicity, polarity, and molecular weight (Tammelin et al., 2015). Surface roughness plays a crucial role in determining the standard of biopolymer films. The degree of roughness

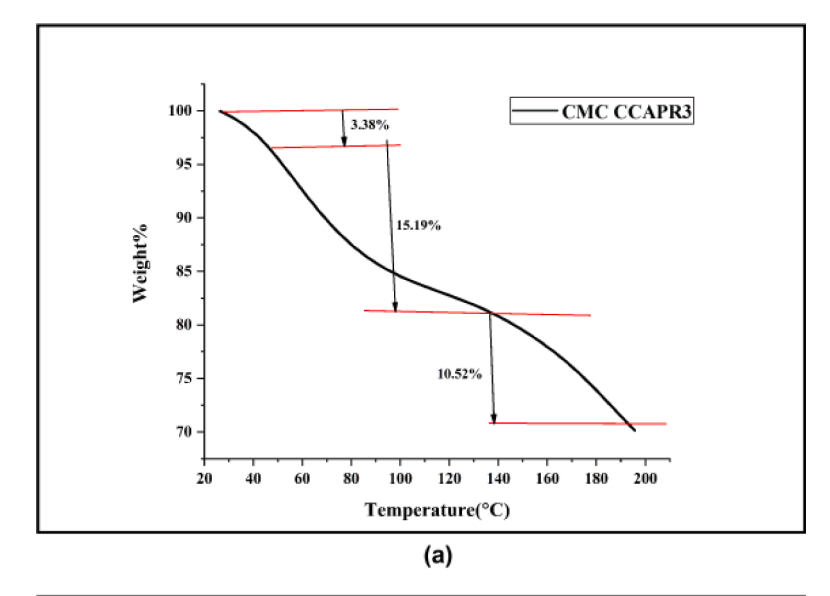
on the cellulose surface directly impacts the bonding strength of the cellulosic film and the plasticizer (Lou et al., 2023).

Overall, the AFM analysis suggests that the incorporation of CCAPL and CCAPR esters as plasticizers in CMC films could offer promising alternatives to conventional plasticizers, with CCAPL ester-containing films demonstrating superior surface morphology compared to CCAPR ester-containing films. The varying surface morphologies observed in the films may be attributed to differences in hydrophobicity, polarity, and molecular weight of the plasticizers (Lou et al., 2023; Mukherjee & Ghosh, 2017).

3.3.4. Mechanical performance of CMC films

The results of the tensile tests conducted on various CMC films are summarized in Table 5. The notably high tensile strength and Young's modulus values, coupled with a low elongation value observed in the control sample, can be attributed to the presence of hydrogen bonds between the CMC chains. These bonds contribute to the high cohesiveness and reduced flexibility of the unplasticized films (Azarifar et al., 2020).

In contrast, CMC films containing glycerol, CCAPL ester, or CCAPR ester exhibited increased elongation properties but decreased tensile strength and Young's modulus with increasing concentrations of glycerol or the respective esters. However, the impact of CCAPL and CCAPR esters on the mechanical properties of the CMC films was more pronounced.



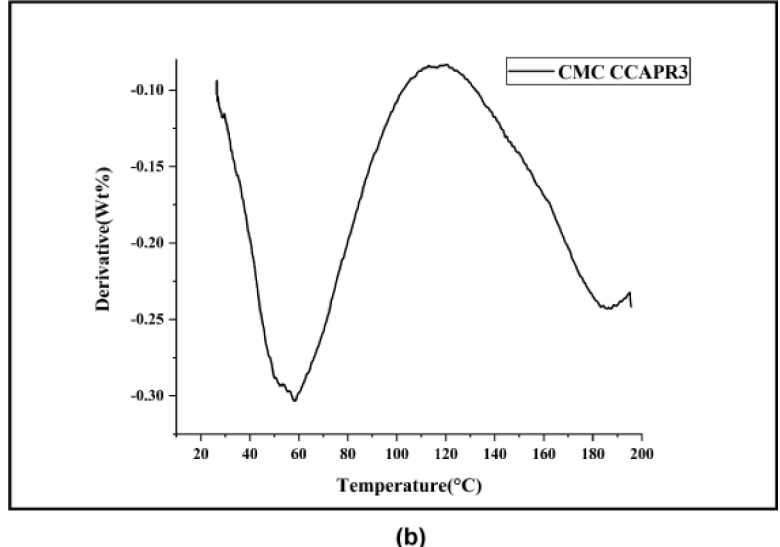


Fig. 11. (a) TG and (b)DTG curves of, pure CMC CCAPR3 film. (For interpretation of the references to color in this figure legend, the reader is referred to the web version of this article.)

For instance, the tensile strength of the pure CMC film was 22.01 MPa for the control (unplasticized) sample, while a significant decrease (p < 0.05) was observed in the case of CMC-CCAPL 3 (2.09 MPa) and CMC-CCAPR 3 (5.17 MPa). Conversely, films containing only glycerol (CMC-GLY) exhibited poor tensile strength, whereas those combining glycerol with CCAPL or CCAPR ester-containing CMC films demonstrated improved mechanical properties. The study is basically focused on the performance of edible plasticizers. Typically, the addition of plasticizers leads to a decrease in the strength of polymeric materials due to the diminished interaction between polymeric chains (Aliotta et al., 2020; Bodaghi, 2020). The incorporation of plasticizers reduces the intermolecular forces along polymer chains, thereby enhancing flexibility and chain mobility. These additives are employed to improve film flexibility, reduce brittleness, and prevent shrinking during handling and storage. Our previous studies showed similar kind of results (Mukherjee & Ghosh, 2017, 2020). Other than that there are several studies found to be observed which support the finding of the present study (Aliotta et al., 2020; Bodaghi, 2020; Chieng et al., 2014).

Numerous packaging materials demand both strong strength properties and considerable elongation at break. However, natural-based polymers often exhibit limited ductility due to the strong hydrogen

bonding between their constituent molecules, resulting in a stiff structure. By modifying the mechanical properties, plasticizers render films more ductile, reduce melt viscosity of the product. Several studies have been reported in the favour of supporting these phenomena (Azarifar et al., 2020; Nazrin et al., 2020; Rivadeneira-Velasco et al., 2021).

Similarly, the modulus property of the films decreased from 580 MPa for the control sample, with CMC-CCAPL 3 showing 70.02 MPa. The impact of CCAPL on the Young's modulus value was less pronounced compared to glycerol, with a value of 90.41 MPa observed for CMC films containing CCAPR (i.e., CMC-CCAPR 3). Thus, the addition of lipid esters (CCAPL/CCAPR) induced the development of a heterogeneous film structure with discontinuities in the polymer network, leading to decreased tensile strength and modulus values alongside increased film flexibility (Acosta et al., 2015; Nisar et al., 2018).

Moreover, the presence of glycerol, coupled with a slight increase in the CCAPL/CCAPR level, resulted in a substantial drop in tensile strength and modulus values, along with a significant increase in elongation properties, as indicated by previous studies (Montero et al., 2017).

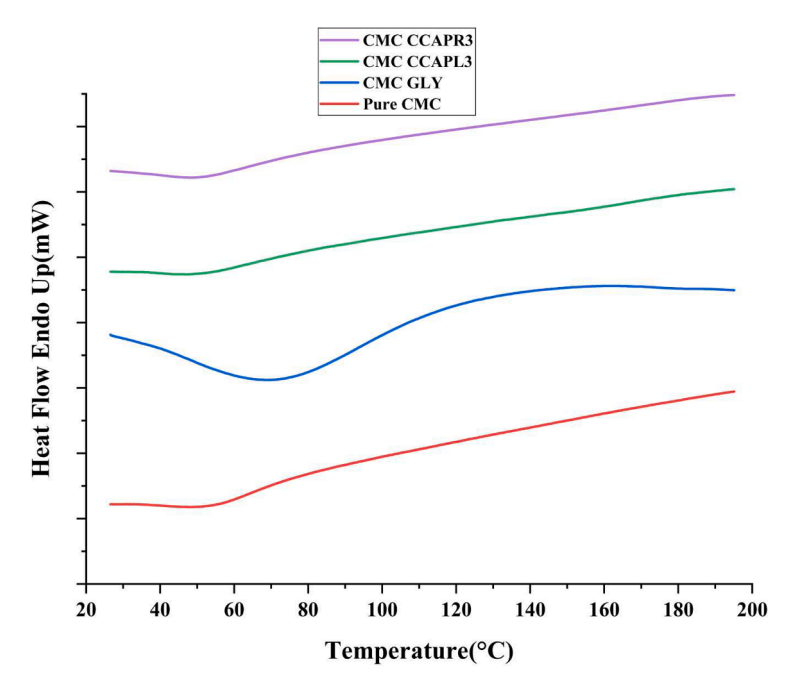


Fig. 12. Comparative DTA curves of, pure CMC, CMC GLY, CMC CCAPL3 and CMC CCAPR3 films. (For interpretation of the references to color in this figure legend, the reader is referred to the web version of this article.)

Table 6Water vapor permeability and moisture absorption properties of CMC film with or without plasticizer.

Sample	Water Vapor permeability (10^{-5} g/ cm ² /24 h)	Moisture Absorption (% w/w)	
Pure CMC	0.85 ± 0.02	40.09 ± 0.1	
CMC-GLY ^a	1.85 ± 0.03	$140.01 \pm 0.2^{\rm d}$	
CMC-CCAPL 1 ^b	1.25 ± 0.01	100.50 ± 0.15	
CMC-CCAPL 2	1.02 ± 0.05	60.05 ± 0.12	
CMC -CCAPL 3	0.42 ± 0.02^{d}	35.08 ± 0.16^e	
CMC-CCAPR 1 ^c	1.39 ± 0.04	125.02 ± 0.2	
CMC- CCAPR	1.34 ± 0.02	80.09 ± 0.15	
2			
CMC-CCAPR 3	0.72 ± 0.04^e	$40.02 \pm 0.12^{\rm f}$	
3			

Values are represented as Mean \pm SEM. n=3.Superscripts (d to f) indicate the significant differences in results (p<0.05) of water vapor permeability and moisture uptake properties of the CMC films.

- ^a CMC-GLY- Carboxymethyl cellulose + glycerol.
- $^{\mathrm{b}}$ CMC-CCAPL- Carboxymethyl cellulose + cetylcaprylate ester.
- $^{\mathrm{c}}$ CMC-CCAPR-Carboxymethyl cellulose + cetylcaprate ester.

3.3.5. Thermal properties

The TG/DTG and DTA data is generated by applying a heating program to the sample. Thermogravimetric Analysis (TGA) involves subjecting a material to heat, leading to the breakdown of bonds within its molecules. This process is crucial for assessing the thermal stability of materials. In differential thermal analysis (DTA), the sample temperature remains steady during endothermic transitions and rises during exothermic transitions. At the same time, a thermogravimetric (TG) curve is plotted, showing the associated mass change. This integrated method provides complementary information, simplifying interpretations compared to using each technique separately (Palermo, 2001).

Curves of TG and DTG studies for pure CMC films and plasticizer added films are presented in Figs. 8-11(a) and (b) respectively.

Thermogravimetric analysis (TGA) stands as a potent technique for assessing the thermal stability of various materials, notably polymers. The TGA curves illustrate a decrease in weight of the films during thermal degradation, while the DTG curves highlight the maximum decomposition temperature at each stage of degradation (Kryszak et al., 2023; Oun & Rhim, 2015). This method involves monitoring changes in a specimen's weight as its temperature rises. Hence a fixed weight of samples for example each sample weighs about 5 mg, which can be assumed as 100 % of the film sample at the initial level of the TGA analysis. In our previous study same phenomena has been reported (Mukherjee & Ghosh, 2017, 2020). Two or three (at least two) distinct weight decreasing steps were evident in the TGA curves for all films during thermal degradation, a characteristic often observed with CMC-based films (El-Sayed et al., 2011; Ghanbarzadeh & Almasi, 2011; Kryszak et al., 2023; Oun & Rhim, 2015). In case of pure CMC film showed (Fig. 8 a) initial mass loss of approximately 2.76 % at the first decomposition step (temperature between 20°C and 40°C) and more substantial mass loss was found to be observed second step which is approximately 10.76 % at a temperature ranging between 40-110 °C (Fig. 8 a). The mass loss was lesser (4.32 %) at the third step of decomposition which was between 110-200 °C (Fig. 8 a). The initial weight decrease, occurring at 20–40 $^{\circ}\text{C},$ primarily resulted from moisture evaporation in the films and the subsequent phase involves CMC degradation (Suripto et al., 2021) .The DTG curve of pure CMC films showed the maximum decomposition between 40-60°C (Fig. 8 b). Higher thermal degradation was detected in case of CMC films containing glycerol (Fig. 9 a), where glycerol was used as conventional edible plasticizers. Here the mass loss of CMC-GLY film was higher in comparison to the pure CMC films and other blended films. CMC-GLY films showed initial mass loss of 5.31 % at temperature between 20–40 $^{\circ}$ C and at the second step of thermal decomposition (40–110 $^{\circ}$ C) the mass loss was 17.07 %, whereas a huge loss of mass was found to be observed in the third step of thermal decomposition (between 110-200 °C) i.e.,55.51 % (Fig. 9 a). The DTG curve of CMC films containing glycerol films showed the maximum decomposition at two major steps such as between 40–60 °C and 180–190 °C (Fig. 9 b). This second phase of weight loss was attributed to the volatilization of glycerol compounds and the thermal degradation of carbohydrate-based polymers. But the trends were slightly decreased when the CMC and glycerol were

combined with CCAPL (Fig. 10 a) and CCAPR (Fig. 11 a) ester respectively as a non-conventional edible plasticizer. CMC-CCAPL3 (Fig. 10 a) and CMC-CCAPR 3 (Fig. 11 a) films showed 2.27 % and 3.38 % of mass loss respectively at the initial thermal decomposition which was almost similar to the pattern of pure CMC films. On the other hand, CMC-CCAPL3 and CMC -CCAPR 3 films exhibited (Figs. 10 a and 11 a) mass loss of 10.03 % and 15.19 % respectively, at the second step of thermal decomposition. Here the decomposition pattern of the CMC-CCAPL 3 film was similar with the pattern of the pure CMC film (Figs. 9a and 10a). Higher amount of mass loss (15.19 %) was found to be observed in case of CMC-CCAPR3 films at the second step of thermal degradation when it was compared with the mass loss (10.03 %) of CMC-CCAPL3 film (Figs. 10a and 11a). The DTG curve of CMC films containing CCAPL and CCAPR ester respectively films showed the maximum decomposition at two major steps such as between 40-60 °C and 180-190 °C (Figs. 10b and 11b). Throughout all stages of thermal degradation, the composite films (CMC-CCAPL3 and CMC-CCAPR 3) exhibited similar or lesser weight loss compared to the control CMC film and CMC-GLY film, indicating higher thermal stability. However, CMC-CCAPR 3 films demonstrated better thermal stability compared to the CMC-GLY films. But better stability was found to be observed in case of CMC films containing CCAPL ester. Enhanced stability is likely due to the superior thermal stability of CMC-CCAPL3 polymer matrix. Similar kind of phenomena was found to be observed oleic acid based CMC film where effect of oleic acid on the CMC not very much impressive (Ghanbarzadeh & Almasi, 2011). But the present research showed positive result in case of CCAPL and CCAPR esters containing CMC films.

The derivative of DTA for CMC reveals two distinct phases of degradation (Fig. 12). Hydroxyl (-OH) group present in the CMC molecule aids in forming strong intermolecular H-bonds. Furthermore, higher plasticizer content might be the cause of the increasing mobility of CMC molecules. Glycerol added sample showed more lowering of the melting point of the CMC films compared to CCAPL and CCAPR ester. This observation might be explained by the varied effect of glycerol and CCAPR/CCAPL ester molecules on H-bonds present amongst the CMC chains. This variation of affinity in turn results in varied segmental mobility (Rivadeneira-Velasco et al., 2021).

When a substance undergoes melting, it absorbs heat from its surroundings. In DTA curves, this absorption of heat is represented as an endothermic peak. This peak is typically sharp and well-defined, indicating the phase transition from solid to liquid. The temperature at which the endothermic peak occurs on the DTA curve corresponds to the melting point of the substance (Palermo, 2001). This temperature is where the solid substance reaches its melting point and begins to transition into a liquid state. In case of differential thermal analytical result, Same trend was also maintained in the case of the CMC films containing CCAPL and CCAPR as non-conventional edible plasticizer. Same pattern of curve was found to be observed in all cases of plasticized and non-plasticized CMC films (Fig. 12).

3.3.6. Water vapor permeability (WVP) and moisture uptake of CMC film WVP observations for pure CMC films and the films with varying amounts of glycerol, CCAPL, and CCAPR contents were presented in Table 6 [Figure S-13 (a) and (b)]. The presence of glycerol, CCAPL, and CCAPR esters led to a difference in the WVP of the pure CMC films. Pure CMC film exhibited the least WVP while the value increased with the addition of glycerol. Water vapors are transmitted mostly by diffusivity and solubility of water molecules through the film matrix. The addition of glycerol molecules in the CMC film escalates the diffusion of water vapor across the film thereby accelerating the transmission of water vapor (Basiak et al., 2018). On the other hand, CMC film containing CCAPL and CCAPR as plasticizers showed the lowest water vapor permeable property and highest barrier properties at their highest concentration in the CMC films. This high hydrophobic nature of CCAPL and CCAPR esters led to this observation. Moreover, immobilization of the polymeric chains with lipid particles added to the medium by

emulsification has increased the barrier properties of the film and reduced the diffusion of water through the interface. This lead to an overall decrease in WVP (Basiak et al., 2018).

Table 6 [Figure S-14 (a) and (b)] described the resultant moisture uptake by the films post conditioning. Glycerol added CMC films showed greater moisture absorption compared to unplasticized counterparts. Being a hydrophilic polymer with medium crystallinity, the cellulose derivatives can reduce the water-absorbing capacity of edible CMC films. Nevertheless, the moisture uptake capacity of CMC films increased with the addition of glycerol. The hydrophilic nature of glycerol promotes its immobilization between CMC chains and leads to the interaction with water molecules. CMC films containing CCAPL and CCAPR esters respectively showed (Table 6) reduced moisture uptake with their use in increased concentration in the CMC films. Additionally, hydrophobic CCAPL/CCAPR esters were able to considerably limit the uptake of moisture by the CMC films even in presence of glycerol, significantly (p < 0.05). Furthermore, immobilization of biopolymer chains by these wax esters results in reduced interaction of water molecules and decreases the overall moisture uptake by the CMC film (Dashipour et al., 2015; Yousuf et al., 2022).

4. Conclusion

Both CCAPL and CCAPR esters were successfully synthesized through lipase-catalyzed esterification reactions, with the NS435 lipase catalyst yielding the highest quantities of both esters. Utilizing an emulsion technique, it is feasible to create CMC-CCAPL or CMC-CCAPR blended films that exhibit enhanced water vapor permeability compared to pure CMC films.

The incorporation of glycerol, CCAPL, and CCAPR significantly influenced the physicochemical properties of the CMC. Increasing glycerol concentration led to a notable decrease in mechanical strength but an increase in water vapor permeability. However, the addition of CCAPL and CCAPR helped reduce the water vapor permeability of the CMC films.

During all stages of thermal degradation, the composite films exhibited similar or lesser weight loss compared to the control CMC film and CMC GLY film, indicating higher thermal stability. Though, CMC CCAPR 3 films demonstrated better thermal stability compared to the CMC-GLY films. But better stability was found to be observed in case of CMC films containing CCAPL ester.

DTA analysis revealed a decrease in temperature for both CMC and plasticized CMC composite films (containing glycerol, CCAPL, and CCAPR). CCAPL and CCAPR had a more pronounced effect on the films' thermal properties compared to glycerol. Thus, its optimal addition is crucial, as it aids in reducing water vapor transmission through CMC films without compromising their mechanical or optical qualities.

The development of CMC films incorporating wax esters holds promise for expanding their utility across various industries in an environmentally friendly manner.

CRediT authorship contribution statement

Sohini Mukherjee: Writing – original draft, Formal analysis, Data curation, Conceptualization. **Avery Sengupta:** Formal analysis, Data curation, Conceptualization. **Subham Preetam:** Writing – review & editing, Writing – original draft, Software, Funding acquisition, Formal analysis, Data curation, Conceptualization. **Tanmoy Das:** Validation, Resources. **Tanima Bhattacharya:** Writing – original draft, Supervision, Project administration, Funding acquisition. **Nanasaheb Thorat:** Supervision, Funding acquisition.

Declaration of competing interest

The authors declare no financial interests/personal relationships which may be considered as potential competing interests.

Data availability

Data will be made available on request.

Acknowledgments

N. D. Thorat, acknowledges funding under the Science Foundation Ireland and Irish Research Council (SFI-IRC) pathway programme (21/ PATH-S/9634). The authors acknowledge the Late Dr. Mahua Ghosh, Associate Professor, Department of Chemical Technology (Oil Technology), University of Calcutta, for her immense support in this study. The entire research work of the present study would have never been possible without her enormous support and immense guidance. The authors would also like to express their gratitude to Professor Dr. Dipak Kumar Bhattacharyya, Ex-Adjunct Professor, School of Community Science and Technology, IIEST, Shibpur, West Bengal, India and Ex-Rashbehari Ghosh Professor and Ex-Emeritus Professor, Department of Chemical Technology, University of Calcutta, West Bengal, India, for his encouragement, constructive ideas and kind advice. The authors also acknowledge S.N. Bose National Centre for Basic Sciences and Center for Research in Nano Science and Nanotechnology and DBT-IPLS, University of Calcutta, for providing facilities to use sophisticated instruments like SEM, AFM, TG/DTA Analyzer, XRD analysis, etc. We further thank Novozyme for the enzyme samples.

Supplementary materials

Supplementary material associated with this article can be found, in the online version, at doi:10.1016/j.carpta.2024.100505.

References

- Acosta, S., Jiménez, A., Cháfer, M., González-Martínez, C., & Chiralt, A. (2015). Physical properties and stability of starch-gelatin based films as affected by the addition of esters of fatty acids. Food Hydrocolloids, 49, 135–143.
- Aggarwal, S., Fatima, A., Shandilya, S., Mangala, B., & Ikram, S. (2024). Covalent immobilization of aspergillus niger lipase on epoxy-activated silver oxide nanoparticles-impregnated chitosan surfaces: characterization, stability & kinetic studies. Catalysis Letters, 1–25.
- Aliotta, L., Vannozzi, A., Panariello, L., Gigante, V., Coltelli, M.-B., & Lazzeri, A. (2020). Sustainable micro and nano additives for controlling the migration of a biobased plasticizer from PLA-based flexible films. *Polymers*, 12(6), 1366.
- Amin, M., Abadi, A. G., Ahmad, N., Katas, H., & Jamal, J. A. (2012). Bacterial cellulose film coating as drug delivery system: Physicochemical, thermal and drug release properties. Sains Malaysiana, 41(5), 561–568.
- Azarifar, M., Ghanbarzadeh, B., & Abdulkhani, A. (2020). The effects of gelatin-CMC films incorporated with chitin nanofiber and trachyspermum ammi essential oil on the shelf life characteristics of refrigerated raw beef. *International Journal of Food Microbiology*, 318, Article 108493.
- Bakry, N. F., Isa, M., & Sarbon, N. M. (2017). Effect of sorbitol at different concentrations on the functional properties of gelatin/carboxymethyl cellulose (CMC)/chitosan composite films. *International Food Research Journal*.
- Balouiri, M., Sadiki, M., & Ibnsouda, S. K. (2016). Methods for in vitro evaluating antimicrobial activity: A review. *Journal of Pharmaceutical Analysis*, 6(2), 71–79.
- Basiak, E., Lenart, A., & Debeaufort, F. (2018). How glycerol and water contents affect the structural and functional properties of starch-based edible films. *Polymers*, 10(4), 412
- Bodaghi, A. (2020). An overview on the recent developments in reactive plasticizers in polymers. *Polymers for Advanced Technologies*, 31(3), 355–367.
- Bozoğlan, B. K., Duman, O., & Tunc, S. (2020). Preparation and characterization of thermosensitive chitosan/carboxymethylcellulose/scleroglucan nanocomposite hydrogels. *International Journal of Biological Macromolecules*, 162, 781–797.
- Carvalho, L. G. G.d., Marques, N.d. N., Fernandes, R.d. S., Villetti, M. A., Souza Filho, M. d. S. M.d., & Balaban, R.d. C. (2021). Effect of starch laurate addition on the properties of mango kernel starch films. *Materials Research*, 24.
- Chieng, B. W., Ibrahim, N. A., Then, Y. Y., & Loo, Y. Y. (2014). Epoxidized vegetable oils plasticized poly (lactic acid) biocomposites: Mechanical, thermal and morphology properties. *Molecules (Basel, Switzerland)*, 19(10), 16024–16038.
- Dahlström, C., Eivazi, A., Nejström, M., Zhang, R., Pettersson, T., Iftikhar, H., Rojas, O. J., Medronho, B., & Norgren, M. (2024). Regenerated cellulose properties tailored for optimized triboelectric output and the effect of counter-tribolayers. Cellulose (London, England), 1–15.
- Dashipour, A., Razavilar, V., Hosseini, H., Shojaee-Aliabadi, S., German, J. B., Ghanati, K., Khakpour, M., & Khaksar, R. (2015). Antioxidant and antimicrobial

- carboxymethyl cellulose films containing Zataria multiflora essential oil. *International Journal of Biological Macromolecules*, 72, 606–613.
- Dmitrenko, M., Kuzminova, A., Cherian, R. M., Joshy, K., Pasquini, D., John, M. J., Hato, M. J., Thomas, S., & Penkova, A. (2023). Edible carrageenan films reinforced with starch and nanocellulose: development and characterization. Sustainability, 15 (22), 15817.
- El-Sayed, S., Mahmoud, K., Fatah, A., & Hassen, A. (2011). DSC, TGA and dielectric properties of carboxymethyl cellulose/polyvinyl alcohol blends. *Physica B:* Condensed Matter, 406(21), 4068–4076.
- Escamilla-García, M., García-García, M. C., Gracida, J., Hernández-Hernández, H. M., Granados-Arvizu, J.Á., Di Pierro, P., & Regalado-González, C. (2022). Properties and biodegradability of films based on cellulose and cellulose nanocrystals from corn cob in mixture with chitosan. *International Journal of Molecular Sciences*, 23(18), 10560.
- Ezati, P., Khan, A., Priyadarshi, R., Bhattacharya, T., Tammina, S. K., & Rhim, J.-W. (2023). Biopolymer-based UV protection functional films for food packaging. Food Hydrocolloids, Article 108771.
- Ghanbarzadeh, B., & Almasi, H. (2011). Physical properties of edible emulsified films based on carboxymethyl cellulose and oleic acid. *International Journal of Biological Macromolecules*, 48(1), 44–49.
- Gibis, M., & Weiss, J. (2017). Inhibitory effect of cellulose fibers on the formation of heterocyclic aromatic amines in grilled beef patties. Food Chemistry, 229, 828–836.
- Hashim, A., & Hamad, Z. S. (2018). Antibacterial activity of biopolymer blend-carbide nanoparticles bio-films against escherichia coli. Research Journal of Agriculture and Biological Sciences, 13(2), 1–5.
- Helmiyati, H., Hidayat, Z. S. Z., Sitanggang, I. F. R., & Liftyawati, D. (2021). Antimicrobial packaging of ZnO-Nps infused into CMC-PVA nanocomposite films effectively enhances the physicochemical properties. *Polymer Testing*, 104, Article 107412.
- Jannatyha, N., Shojaee-Aliabadi, S., Moslehishad, M., & Moradi, E. (2020). Comparing mechanical, barrier and antimicrobial properties of nanocellulose/CMC and nanochitosan/CMC composite films. *International Journal of Biological Macromolecules*, 164, 2323–2328.
- Karami, A., Ghanbarzadeh, B., Fakhri, L. A., Falcone, P. M., & Hosseini, M. (2023). Physico-mechanical optimization and antimicrobial properties of the bionanocomposite films containing gallic acid and zinc oxide nanoparticles. *Nanomaterials*, 13(11), 1769.
- Khan, A., Priyadarshi, R., Bhattacharya, T., & Rhim, J.-W. (2023). Carrageenan/alginate-based functional films incorporated with Allium sativum carbon dots for UV-barrier food packaging. Food and Bioprocess Technology, 16(9), 2001–2015.
- Kryszak, B., Biernat, M., Tymowicz-Grzyb, P., Junka, A., Brożyna, M., Worek, M., Dzienny, P., Antończak, A., & Szustakiewicz, K. (2023). The effect of extrusion and injection molding on physical, chemical, and biological properties of PLLA/HAp whiskers composites. *Polymer*, 287, Article 126428.
- Liu, J., Cui, L., Shi, Y., Zhang, Q., Zhuang, Y., & Fei, P. (2022). Preparation of hydrophobic composite membranes based on carboxymethyl cellulose and modified pectin: Effects of grafting a long-chain saturated fatty acid. *International Journal of Biological Macromolecules*, 222, 2318–2326.
- Liu, Z., Shen, R., Yang, X., & Lin, D. (2021). Characterization of a novel konjac glucomannan film incorporated with pickering emulsions: Effect of the emulsion particle sizes. *International Journal of Biological Macromolecules*, 179, 377–387.
- Lou, Z., Zhang, Y., Li, Y., & Xiao, H. (2023). Study on microscopic physical and chemical properties of biomass materials by AFM. *Journal of Materials Research and Technology*.
- Montero, B., Rico, M., Rodríguez-Llamazares, S., Barral, L., & Bouza, R. (2017). Effect of nanocellulose as a filler on biodegradable thermoplastic starch films from tuber, cereal and legume. *Carbohydrate Polymers*, 157, 1094–1104.
- Mukherjee, S., & Ghosh, M. (2017). Studies on performance evaluation of a green plasticizer made by enzymatic esterification of furfuryl alcohol and castor oil fatty acid. Carbohydrate Polymers, 157, 1076–1084.
- Mukherjee, S., & Ghosh, M. (2020). Performance evaluation and biodegradation study of polyvinyl chloride films with castor oil-based plasticizer. *Journal of the American Oil Chemists' Society*, 97(2), 187–199.
- Nazrin, A., Sapuan, S., Zuhri, M., Ilyas, R., Syafiq, R., & Sherwani, S. (2020).
 Nanocellulose reinforced thermoplastic starch (TPS), polylactic acid (PLA), and polybutylene succinate (PBS) for food packaging applications. Frontiers in Chemistry, 8, 213.
- Nisar, T., Wang, Z.-C., Yang, X., Tian, Y., Iqbal, M., & Guo, Y. (2018). Characterization of citrus pectin films integrated with clove bud essential oil: Physical, thermal, barrier, antioxidant and antibacterial properties. *International Journal of Biological Macromolecules*, 106, 670–680.
- Oun, A. A., & Rhim, J.-W. (2015). Preparation and characterization of sodium carboxymethyl cellulose/cotton linter cellulose nanofibril composite films. *Carbohydrate Polymers*, 127, 101–109.
- Palermo, P. J. (2001). Solid dosage-form analysis. Handbook of modern pharmaceutical analysis (pp. 235–267). San Diego: Academic Press.
- Paudel, S., Regmi, S., & Janaswamy, S. (2023). Effect of glycerol and sorbitol on cellulose-based biodegradable films. Food Packaging and Shelf Life, 37, Article 101090.
- Rahman, M. S., Hasan, M. S., Nitai, A. S., Nam, S., Karmakar, A. K., Ahsan, M. S., Shiddiky, M. J., & Ahmed, M. B. (2021). Recent developments of carboxymethyl cellulose. *Polymers*, 13(8), 1345.
- Rivadeneira-Velasco, K. E., Utreras-Silva, C. A., Díaz-Barrios, A., Sommer-Márquez, A. E., Tafur, J. P., & Michell, R. M. (2021). Green nanocomposites based on thermoplastic starch: A review. *Polymers*, *13*(19), 3227.

- Roy, N., Saha, N., Kitano, T., & Saha, P. (2010). Novel hydrogels of PVP–CMC and their swelling effect on viscoelastic properties. *Journal of Applied Polymer Science*, 117(3), 1703–1710.
- Roy, S., & Rhim, J.-W. (2020). Carboxymethyl cellulose-based antioxidant and antimicrobial active packaging film incorporated with curcumin and zinc oxide. *International Journal of Biological Macromolecules*, 148, 666–676.
- Suripto, S., Noviany, N., Wasinton, S., Kiswandono, A.A., & Sutopo, H. (2021). Similarity characterization of carboxymethyl cellulose (CMC) synthesized from microcellulose of cassava peel.
- Tammelin, T., Abburi, R., Gestranius, M., Laine, C., Setälä, H., & Österberg, M. (2015).
 Correlation between cellulose thin film supramolecular structures and interactions with water. Soft Matter, 11(21), 4273–4282.
- Tyagi, V., & Thakur, A. (2023). Applications of biodegradable carboxymethyl cellulosebased composites. *Results in Materials*, Article 100481.
- Vilas Boas, R. N., & de Castro, H. F. (2022). A review of synthesis of esters with aromatic, emulsifying, and lubricant properties by biotransformation using lipases. *Biotechnology and Bioengineering*, 119(3), 725–742.
- Yousuf, B., Sun, Y., & Wu, S. (2022). Lipid and lipid-containing composite edible coatings and films. *Food Reviews International, 38*(sup1), 574–597.
- Zhu, J., Li, Q., Che, Y., Liu, X., Dong, C., Chen, X., & Wang, C. (2020). Effect of Na2CO3 on the microstructure and macroscopic properties and mechanism analysis of PVA/CMC composite film. *Polymers*, 12(2), 453.